Eur. Phys. J. D **13**, 361–365 (2001)

THE EUROPEAN
PHYSICAL JOURNAL D
EDP Sciences

Fragmentation of water clusters: Molecular-dynamics simulation study

Ş. Erkoç[1,a], H. Kökten[1], and Z. Güvenç[2]

[1] Department of Physics, Middle East Technical University, 06531 Ankara, Turkey
[2] Department of Computer Engineering, Çankaya University, 06530 Ankara, Turkey

Received 27 April 2000 and Received in final form 6 October 2000

Abstract. The fragmentation of water clusters, $[(H_2O)_n;\ n = 2–8]$, have been investigated by using molecular-dynamics simulation method. In the simulations a polarizable-dissociable potential energy function for water has been used. Particular attention has bee paid to investigate the effect of structural properties and cluster size on the fragmentation.

PACS. 36.40.Qv Stability and fragmentation of clusters – 61.46.+w Clusters, nanoparticles, and nanocrystalline materials – 31.15.Qg Molecular dynamics and other numerical methods

1 Introduction

Water is the most commonly used solvent in chemistry and yields strong solvent effects on reactions. It also acts as a very efficient energy absorber in the relaxation processes of photochemical reactions. To understand these and other solvent effects, a detailed knowledge of static and dynamical properties of water in the molecular level is required [1]. The properties of water are of widespread and continuing interest [2]. Much of this interest is due to the role that it plays in not only physical chemistry but also biology and atmospheric science [3]. The detailed study of water clusters should, therefore, contribute to a wide range of chemical problems including structure of condensed phases, solvation, intramolecular structure, and many areas of biochemistry involving hydrogen bonding [4].

Scientists have long realised that water clusters could test the usefulness of water-interaction models for environments other than bulk water [5]. Water clusters have been directly implicated in several other contemporary problems, including the formation of acid rain, the anomalous absorption of sunlight by clouds, the nucleation of water droplets, and the formation of microemulsions [6,7]. The condensation of water droplets has been studied for many years. It is of especial interest in atmospheric problems concerning the formation of clouds and aerosols [8].

Although there are many studies on the structural properties of water clusters [6,9–27], a less attention was paid to the fragmentation of water clusters. There are only a few works about the dissociation of water clusters [23,24,28,29]. Fragmentation of atomic and molecular clusters is a well studied phenomenon, however it has received relatively less attention from the theoretical side. This is especially true for molecular systems. The fragmentation of clusters, in general, gives information about the size distribution and mass selective detection as well as the velocity distribution of the fragments and the translational energy released in the predissociation [29]. This type of information is important for the experimental studies. In the present work we have studied systematically the fragmentation of water clusters containing upto eight molecules.

2 The method of calculation

In the present work we have studied the molecular-dynamics simulations of the fragmentation of water clusters, $(H_2O)_n;\ n = 2–8$, by using a polarizable-dissociable (PD) many-body empirical potential energy function developed for liquid water [9]. There are several potential energy functions proposed for water clusters, such as CF type [30–33], TIP type [34], ST type [35], BF type [36], SPC type [37], CKL type [38], and NCC type [39] potentials, and *ab initio* calculations are also possible for small water-cluster [23,24]. The potential energy function (PEF) used in this work, namely PD type PEF comprises also many-body effects and reproduces the structural features of water clusters predicted by *ab initio* calculations. The total potential energy of a water dimer in this model is given as [9]:

$$\phi = \phi_{\mathrm{HH}} + \phi_{\mathrm{OH}} + \phi_{\mathrm{OO}} + \phi_{\mathrm{OH-md}} + \phi_{\mathrm{OO-md}} + \phi_{\mathrm{OO-dd}} + \phi_{\mathrm{mol}}. \quad (1)$$

The first three terms represent the two-body interactions, the forth and the fifth terms represent the monopole-dipole interactions, the sixth term represents

---

[a] e-mail: `erkoc@erkoc.physics.metu.edu.tr`

Table 1. Parameters of the potential energy function used in the simulations [9].

$h_1 = 143.99$ eV Å^{-1}	$m_1 = -9.2217$ eV Å^{-2}	$f_1 = 1.28$ Å	$s_{\mathrm{md}} = 0.3$ Å^2
$h_2 = 3.6994$ Å^{-1}	$m_2 = 0.28114$ eV rad^{-2}	$f_2 = 0.01$ Å^{-1}	$a_{\mathrm{md}} = 1.1$ Å^{-1}
$h_3 = -5.9248$ eV Å^{-2}	$m_3 = -5.0094$ eV Å^{-1} rad^{-1}	$f_3 = 121.26$ Å^2	$s_{\mathrm{dd}} = 0.1$ Å^2
$h_4 = 1.6248$ eV Å^{-1}	$m_4 = -0.31138$ eV rad^{-1}	$f_4 = 4.71$ Å^{-1}	$a_{\mathrm{dd}} = 1.2$ Å^{-1}
$h_5 = 16.000$ Å^{-2}	$m_5 = 16.0$ Å^{-2}		
$A = 2.5602$ eV Å^{12}			
$B = 2.105$ eV Å^6			
$\alpha = 1.444$ Å^3			

the dipole-dipole interaction, and the last term represents the three-body interaction. The explicit form of these terms are as follows [9]:

$$\phi_{\mathrm{HH}} = \frac{e^2}{r}, \tag{2}$$

$$\phi_{\mathrm{OH}} = \frac{h_1}{r}\mathrm{e}^{-h_2 r} - \frac{2e}{r} + [h_3(r-r_e)^2 - h_4(r-r_e)] \times \mathrm{e}^{-h_5(r-r_e)^2}, \tag{3}$$

$$\phi_{\mathrm{OO}} = \frac{4e^2}{r} + \frac{A}{r^{12}} - \frac{B}{r^6}, \tag{4}$$

$$\phi_{\mathrm{OH-md}} = -\sum_{\mathrm{H}} q_{\mathrm{H}} \sum_{\mathrm{O}} \frac{\mu_{\mathrm{O}} \cdot \mathbf{r}_{\mathrm{OH}}}{r_{\mathrm{OH}}^3} S_{\mathrm{OH}}(r_{\mathrm{OH}}), \tag{5}$$

$$\phi_{\mathrm{OO-md}} = -\sum_{\mathrm{O}} q_{\mathrm{O}} \sum_{\mathrm{O'} \neq \mathrm{O}} \frac{\mu_{\mathrm{O}} \cdot \mathbf{r}_{\mathrm{OO'}}}{r_{\mathrm{OO'}}^3} S_{\mathrm{OO}}^{\mathrm{md}}(r_{\mathrm{OO'}}), \tag{6}$$

$$\phi_{\mathrm{OO-dd}} = \frac{1}{2}\sum_{\mathrm{O}} \sum_{\mathrm{O'} \neq \mathrm{O}} \frac{\mu_{\mathrm{O}} \cdot \mathbf{T}_{\mathrm{OO'}} \cdot \mu_{\mathrm{O'}}}{r_{\mathrm{OO'}}^3} S_{\mathrm{OO}}^{\mathrm{dd}}(r_{\mathrm{OO'}}), \tag{7}$$

$$\phi_{\mathrm{mol}} = [m_1(r_1-r_e)(r_2-r_e) + \frac{1}{2}m_2(\theta-\theta_e)^2 + m_3(\theta-\theta_e)(r_1+r_2-2r_e) + m_4(\theta-\theta_e)] \times \mathrm{e}^{-m_5[(r_1-r_e)^2+(r_2-r_e)^2]}. \tag{8}$$

The cutoff functions, S, are expressed as

$$S_{\mathrm{OH}}(r) = \frac{r^2}{r^2 + f_{\mathrm{OH}}(r)}, \quad f_{\mathrm{OH}}(r) = f_1(r-r_e)\mathrm{e}^{-f_2(r-r_e)} + f_3\mathrm{e}^{-f_4 r}, \tag{9}$$

$$S_{\mathrm{OO}}^{\mathrm{md}}(r) = \frac{r^2}{r^2 + f_{\mathrm{OO}}^{\mathrm{md}}(r)}, \quad f_{\mathrm{OO}}^{\mathrm{md}}(r) = s_{\mathrm{md}}\mathrm{e}^{-a_{\mathrm{md}} r}, \tag{10}$$

$$S_{\mathrm{OO}}^{\mathrm{dd}}(r) = \frac{r^2}{r^2 + f_{\mathrm{OO}}^{\mathrm{dd}}(r)}, \quad f_{\mathrm{OO}}^{\mathrm{dd}}(r) = s_{\mathrm{dd}}\mathrm{e}^{-a_{\mathrm{dd}} r}. \tag{11}$$

The dyadic tensor, $\mathbf{T}$, is defined as

$$\mathbf{T}_{\mathrm{OO'}} = \mathbf{I} - 3\frac{\mathbf{r}_{\mathrm{OO'}}\mathbf{r}_{\mathrm{OO'}}}{r_{\mathrm{OO'}}^2} \cdot \tag{12}$$

In this model potential the hydrogen atoms are regarded as bare protons having zero polarizability while the oxygens are regarded as doubly charged anions with a polarizability of 1.444 Å^3. The dipole moments, μ_{O}, are considered as dynamical variables and have kinetic and potential energies. The parameters of the potential energy function used in the simulations are given in Table 1. The details of the method of parameterization for the present potential energy function may be found in [9].

Dissociation of molecules strongly depends on the interatomic and intermolecular forces, therefore molecules having permanent dipole moment, such as water molecules, should be described by a realistic PEF. The present PEF satisfies all the requirements, therefore we have preferred this PEF in the present simulations. The present calculations have been performed by molecular-dynamics simulation, which was based on microcanonical ensemble (NVE) molecular dynamics [40]. The equations of motion of the particles are solved by the Verlet algorithm [40] with the step size of 10^{-16} s.

In the simulations we have investigated the fragmentation of water clusters systematically by considering two sets of clusters: one set is formed from the clusters in their global minimum configuration, and the other set is formed from the clusters in their local minimum configurations. We have started from various initial configurations and the one with minimum energy was selected as global minimum configuration, the stable configurations with higher energies were assumed to be local minimum configurations. We have to do this procedure; it may not be possible to reach global minimum configuration in a single choice of initial geometry. The stable geometries, of course, depend on the PEF used in the simulations. Different PEFs may give different geometries as global and/or local minimum configuration. The global minimum geometries obtained in this study are in agreement with the literature data [15]. We have selected the local minimum configurations such that the geometry of the cluster considered is different than that of the global minimum geometry. By choosing two sets of clusters we aim to get information of the effect of initial configuration to the fragmentation of water clusters. We have considered the water clusters of the sizes $(H_2O)_n$; $n = 2-8$ for both sets.

During the simulation the temperature of each cluster is kept fixed. Keeping the temperature constant causes the system to change its configuration. The initial temperature of the system was taken as 1 K and increased by 50 K steps until the cluster is fragmented (or dissociated). The clusters are simulated for 150 000 time steps at every temperature raise. The initial structures of the water clusters considered are given in Figures 1 and 2.

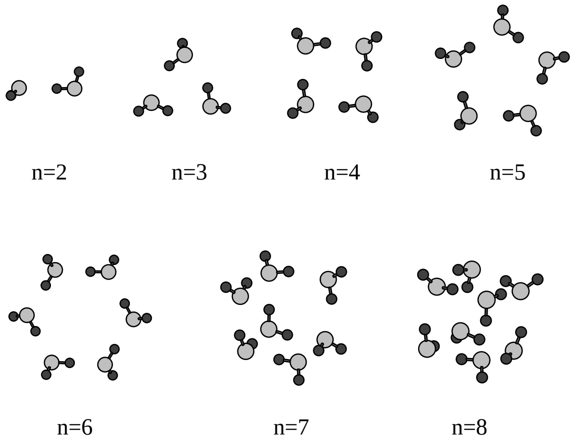

Fig. 1. Geometries of water clusters in their global minimum configurations.

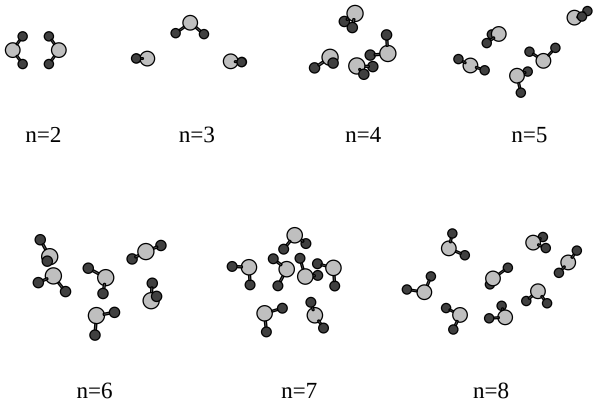

Fig. 2. Geometries of water clusters in their local minimum configurations.

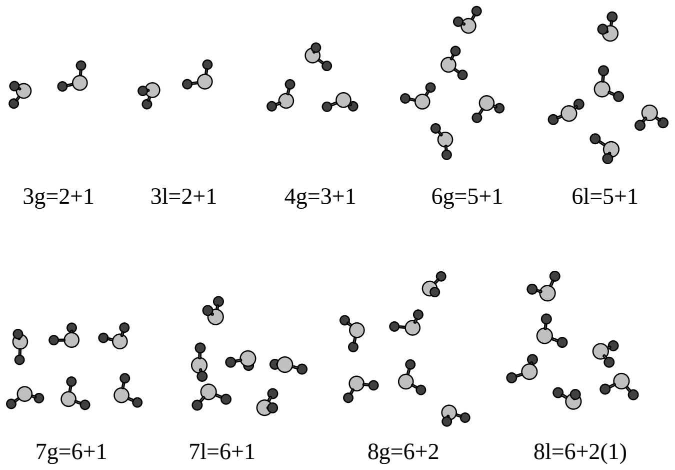

Fig. 3. Geometries of water clusters after fragmentation.

For each starting configuration we performed only one simulation. We did not repeat the simulations for statistical averages and/or rate processes, which is a different subject of interest.

Table 2. The fragmentation channels (type of the dissociation) and the temperature range (in Kelvin) for fragmentation both from global minimum structure (denoted by g) and from local minimum structure (denoted by l) of water clusters $(H_2O)_n$.

n	(g)		(l)	
2	$1+1$ (md);	100−150	$1+1$ (md);	100−150
3	$2+1$ (md);	100−150	$2+1$ (md);	100−150
4	$3+1$ (md);	150−200	4×1 (ed);	150−200
5	5×1 (ed);	100−150	5×1 (ed);	200−250
6	$5+1$ (md);	200−250	$5+1$ (md);	200−250
7	$6+1$ (md);	200−250	$6+1$ (md);	200−250
8	$6+2$ (cd);	200−250	$6+2\times1$ (mmd);	200−250

3 Results and discussion

Fragmentation of a cluster, in general, may take place as one of the following four possible channels:

- Monomer dissociation (md): $X_n = X_{n-1} + X$; $n \geq 2$,
- Multimonomer dissociation (mmd):
  $X_n = X_{n-m} + mX$; $m \geq 2$, $n \geq 4$, $n > m$,
- Explosive dissociation (ed): $X_n = nX$; $n \geq 3$,
- Cluster dissociation (cd):
  $X_n = X_{n-m} + X_m$; $m \geq 2$, $n \geq 4$, $n > m$.

In the present simulations all these possible dissociation channels took place for the water clusters considered. The fragmentation channels and the temperature range for the clusters considered in the present calculations are given in Table 2.

The total potential energy of the clusters and their fragments are given in Table 3. We may also call the fragmentation energy as the binding energy or dissociation energy of the cluster. The fragmentation energy (E_f) can easily be obtained from the fragmentation channel reaction equations expressed above as the following:

- Monomer dissociation: $E_\mathrm{f} = E_n - E_{n-1} - E_1$,
- Multimonomer dissociation: $E_\mathrm{f} = E_n - E_{n-m} - mE_1$,
- Explosive dissociation: $E_\mathrm{f} = E_n - nE_1$,
- Cluster dissociation: $E_\mathrm{f} = E_n - E_{n-m} - E_m$.

The fragmentation energies calculated from the present simulations are given in Table 4. Water dimer dissociates as monomer type into two water molecules in the temperature range 100−150 K from both global minimum and local minimum configurations as expected. Water trimer dissociates as monomer type into dimer and monomer in the temperature range 100−150 K from both global and local minimum configurations. Water tetramer dissociates as monomer type into trimer and monomer from global minimum configuration, and as explosive type into four monomers from local minimum configuration. The temperature range for both tetramers is 150−200 K. Water pentamer dissociates as explosive type into five monomers both from global minimum in the temperature range 100−150 K, and from local minimum in the temperature range 200−250 K. Water hexamer dissociates as monomer type into pentamer and monomer in

Table 3. Total potential energy (in eV) of water clusters $(H_2O)_n$ and their corresponding fragments. The clusters initially in their global minimum structure are labeled by g, and in their local minimum structure are labeled by l. The numbers in the parenthesis represent the size of the largest fragment after dissociation. The total potential energy of a single water molecule (monomer) is −44.84788 eV.

n	$E_{\rm g}$	$E_{\rm l}$	$E_{\rm f}^{\rm g}(q)$	$E_{\rm f}^{\rm l}(q)$	$E_{\rm f}^{\rm g}(f)$	$E_{\rm f}^{\rm l}(f)$
2	−90.02548	−90.00101	—	—	—	—
3	−135.35508	−135.20871	−134.84298	−134.84801	−89.99640(2)	−75.39701(2)
4	−180.94707	−180.86301	−180.17445	−179.38255	−135.32817(3)	—
5	−226.29797	−226.20279	−224.22955	−224.22926	—	—
6	−271.61073	−271.59778	−270.94463	−270.87108	−197.85798(5)	−226.11000(5)
7	−316.91515	−316.85714	−316.23133	−315.37927	−243.09877(6)	−271.47760(6)
8	−362.47576	−360.93700	−361.21191	−360.99630	−271.23061(6) −89.98172(2)	−248.85367(6)

Table 4. Fragmentation energy (in eV) of water clusters $(H_2O)_n$. The primed values are obtained from the total potential energy of the fragments.

n	$E_{\rm f}^{\rm g}$	$E_{\rm f}^{\rm l}$	$E_{\rm f}^{\rm g'}$	$E_{\rm f}^{\rm l'}$
2	−0.32974	−0.30528	—	—
3	−0.48173	−0.33536	−0.51080	−14.96382
4	−0.74412	−1.47154	−0.77103	—
5	−2.05863	−1.96364	—	—
6	−0.46489	−0.54693	−28.90489	−0.63789
7	−0.45654	−2.92206	−28.96850	−0.53167
8	−0.83954	+0.35651	−1.26341	−22.38759

the temperature range 200−250 K from both global and local minimum configurations. Water heptamer dissociates as monomer type into hexamer and monomer in the temperature range 200−250 K from both global and local minimum configurations. Water octamer dissociates as cluster type in the temperature range 200−250 K from global minimum configuration, and as multimonomer type in the temperature range 200−250 K from local minimum configuration. The variation of average energies per water molecule as a function of temperature are shown in Figures 4 and 5 for the water clusters initially in their global and local minimum configurations, respectively. The rapid change in energy corresponds to the dissociation; we consider the corresponding temperature as the upper limit for fragmentation.

Ahmed *et al.* [28] in their experimental work observed that the majority of dissociation of water clusters take place as monomer type. In the present simulation we have also obtained the majority of dissociation of water clusters as monomer type. Although Ahmed *et al.*'s experimental work deals with large water clusters, it is interesting to get similar results in small water clusters. Gregory and Clary [23] calculated the dissociation of water trimer as monomer type. Vernon *et al.* [29] in their experimental work pointed out that water clusters may dissociate either in monomer type and cluster type; they also performed a model calculation (without relaxation) for the dissociation of water dimer, trimer and tetramer as monomer type.

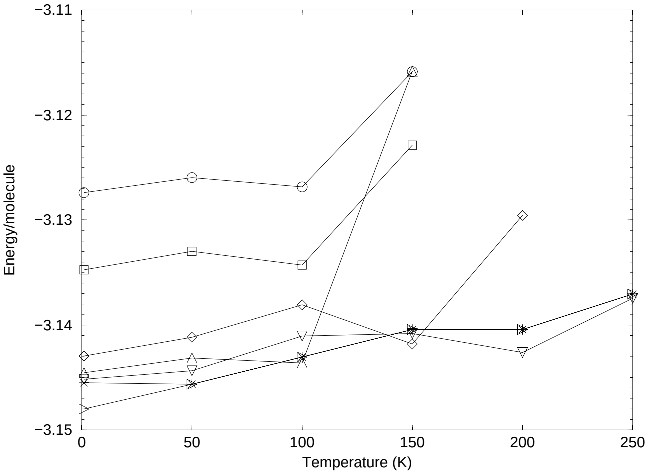

Fig. 4. Variation of energy (1 unit = 14.393 eV) per molecule as a function of temperature for the water clusters initially in their global minimum configurations. Circle ($n = 2$), square ($n = 3$), diamond ($n = 4$), triangle-up ($n = 5$), triangle-down ($n = 6$), star ($n = 7$), triangle-right ($n = 8$).

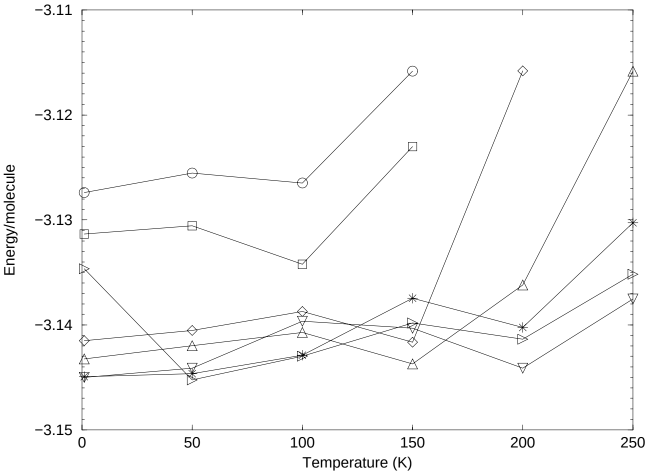

Fig. 5. Variation of energy (1 unit = 14.393 eV) per molecule as a function of temperature for the water clusters initially in their local minimum configurations. Circle ($n = 2$), square ($n = 3$), diamond ($n = 4$), triangle-up ($n = 5$), triangle-down ($n = 6$), star ($n = 7$), triangle-right ($n = 8$).

When water clusters dissociate the geometry of the fragments (not that of the monomers) are not in their global minimum structure. The geometries of the fragments after dissociation are given in Figure 3. The temperature range in fragmentation is the same for both clusters in their global minimum and local minimum structure. There is an exception for the water pentamer; water pentamer in its local minimum configuration dissociates relatively at higher temperature with respect to the water pentamer in its global minimum configuration. One expects that clusters in their local minimum structure dissociate easily with respect to the corresponding global minimum structure.

References

1. I. Ohmine, H. Tanaka, P.G. Wolynes, J. Chem. Phys. **89**, 5852 (1988).
2. I.R. McDonald, M.L. Klein, J. Chem. Phys. **68**, 4875 (1978).
3. R.S. Taylor, L.X. Dang, B.C. Garrett, J. Phys. Chem **100**, 11720 (1996).
4. T.R. Dyke, K.M. Mack, J.S. Muenter, J. Chem. Phys. **66**, 498 (1977).
5. `http://www.psc.edu/MetaCenter/MetaScience/Articles/Jordan/TakingBath.html`
6. K. Liu, J.D. Cruzan, R.J. Saykally, Science **271**, 929 (1996).
7. E.N. Brodskaya, J.C. Eriksson, A. Laaksonen, A.I. Rusanov, J. Colloid Interf. Sci. **180**, 86 (1996).
8. C.L. Briant, J.J. Burton, J. Chem. Phys. **63**, 3327 (1975).
9. J.W. Halley, J.R. Rustad, A. Rahman, J. Chem. Phys. **98**, 4110 (1993).
10. P. Barnes, J.L. Finney, J.D. Nicholas, J.E. Quinn, Nature **282**, 459 (1979).
11. J.R. Reimers, R.O. Watts, Chem. Phys. **85**, 83 (1984).
12. D. Belford, E.S. Campbell, J. Chem. Phys. **86**, 7013 (1987).
13. S.C. Farantos, S. Kapetanakis, A. Vegiri, J. Phys. Chem. **97**, 12158 (1993).
14. B. J. Mhin, J. Kim, S. Lee, J. Y. Lee, K. S. Kim, J. Chem. Phys. **100**, 4484 (1994).
15. Z.B. Güvenç, M.A. Anderson, Z. Phys. D **36**, 171 (1996).
16. D.J. Wales, Science **271**, 925 (1996).
17. J.K. Gregory, D.C. Clary, J. Phys. Chem. **100**, 18014 (1996).
18. L.S. Sremaniak, L. Perera, M.L. Berkowitz, J. Chem. Phys. **105**, 3715 (1996).
19. M. Masella, J.P. Flament, J. Chem. Phys. **107**, 9105 (1997).
20. A. Khan, J. Phys. Chem. A **103**, 1260 (1999).
21. J. Sadlej, V. Buch, J.K. Kazimirski, U. Buck, J. Phys. Chem. A **103**, 4933 (1999).
22. K.P. Schröder, Chem. Phys. **123**, 91 (1988).
23. J.K. Gregory, D.C. Clary, J. Chem. Phys. **103**, 8924 (1995).
24. J.K. Gregory, D.C. Clary, J. Phys. Chem. **100**, 18014 (1996).
25. J. Pillardy, K.A. Olszewski, L. Piela, J. Mol. Struct. **270**, 277 (1992).
26. D.J. Wales, M.P. Hodges, Chem. Phys. Lett. **286**, 65 (1998).
27. Ş. Erkoç, E. Güneyler, Physica E **8**, 40 (2000).
28. M. Ahmed, C.J. Apps, C. Hughes, J.C. Whitehead, J. Phys. Chem. **98**, 12530 (1994).
29. M.F. Vernon, D.J. Krajnovick, H.S. Kwok, J.M. Lisy, Y.R. Shen, Y.T. Lee, J. Chem. Phys. **77**, 47 (1982).
30. H.L. Lemberg, F.H. Stillinger, J. Chem. Phys. **62**, 1677 (1975).
31. F.H. Stillinger, A. Rahman, J. Chem. Phys. **68**, 666 (1978).
32. A. Rahman, F.H. Stillinger, H.L. Lemberg, J. Chem. Phys. **63**, 5223 (1975).
33. P. Bopp, G. Jancso, K. Heinzinger, Chem. Phys. Lett. **98**, 129 (1983).
34. W.L. Jorgensen, J. Chandrasekhar, J.D. Madura, J. Chem. Phys. **79**, 926 (1983).
35. F.H. Stillinger, A. Rahman, J. Chem. Phys. **60**, 1545 (1974).
36. J.D. Bernal, R.H. Fowler, J. Chem. Phys. **1**, 515 (1933).
37. H.J.C. Berenosen, J.P.M. Postma, W.F. van Gunsteren, J. Hermans, *Intermolecular Forces*, edited by B. Pullman (Dordrecht Reidel, 1981), p. 331.
38. P. Cieplak, P. Kollman, T. Lybrand, J. Chem. Phys. **92**, 6755 (1990).
39. U. Niesar, G. Corongiu, E. Clementi, G.R. Kneller, D.K. Bhattacharya, J. Phys. Chem. **34**, 7949 (1990).
40. D.W. Heermann, *Computer Simulation Methods in Theoretical Physics* (Springer-Verlag, 1990).